IL NUOVO CIMENTO VOL. 14 C, N. 6 Novembre-Dicembre 1991

Merging of Barotropic Symmetric Vortices. A Case Study for Gulf Stream Rings.

S. MASINA and N. PINARDI
Istituto per lo Studio delle Metodologie Geofisiche Ambientali, CNR - Modena, Italia

(ricevuto il 18 Gennaio 1990; approvato il 10 Maggio 1991)

Summary. — We made numerical experiments to study the merging dynamics of axisymmetric barotropic ringlike vortices using a quasi-geostrophic model in a β-plane. We want to explore the initial conditions and the physical parameters that cause the merging or that affect the merging rates of ringlike structures. The initial vortices have a «realistic» shape, *i.e.*, they are taken to simulate closely the horizontal structure of Gulf Stream rings. In the first set of experiments we change the initial conditions. The results agree with the classical solution that there is a critical initial separation distance d between the two vortices: for bigger merging distances the process cannot occur. The initial distance affects the merging rates and it determines the development of the lateral arms and the behaviour of the «near-field» vortices. The latter form near the elongated arms of the merging vortices; sometimes the arms of the merged vortex become unstable and get detached from the central merged vorticity region to form dipolar structures with «near-field» vortices. A second set of numerical simulations is done by changing the numerical model parameters. The results show that the merging is a nonlinear process very sensitive to the value of the nonlinear parameter, α, and that the β-effect does not alter appreciably the speed of merging but it affects the development of the arms.

PACS 92.10 – Physics of the oceans.

1. – Introduction.

An experiment made by Robinson *et al.* [1] in the Northeast Pacific provided a real example of the merger of two oceanic mesoscale eddies. In recent years a lot of numerical and analytical studies have been made about interactions between isolated vortices. But in spite of the importance of the merger process, there has so far been only a limited understanding of the nonlinear dynamics of interacting oceanic vortices.

Christiansen and Zabusky [2] made computational experiments to study the stability and long-time evolution of two-dimensional uniform vorticity patches in incompressible inviscid fluids. In this case the critical parameter is b/a, the initial transverse-to-longitudinal separation ratio of the vortex centres. Systems with b/a greater than a critical value are unstable and like-signed regions of vorticity attract and final-

ly *fuse*. Overman and Zabusky [3] studied numerical simulations of the instability, merger, and breaking of two piecewise-constant finite-area vortex regions. A contour dynamical algorithm is used. They show that the inviscid merger process may be viewed as the long-time behaviour of the evolution of an *instability* of the perturbed vortex regions. Symmetric vortex regions were found to be unstable when properly perturbed if their centroid-effective radius ratio, $\overline{x}/R$, is less than a critical value. This causes the vortex regions to approach at an exponential rate, merge, and reform into a stable elliptical structure with filamentary arms or tails (to conserve angular momentum). Similar results have been obtained by Melander *et al.* [4] who examined the merging of two identical regions of uniform vorticity using an approximation to the 2D-Euler equations. Using an analytical model, they obtained a necessary and sufficient condition for merger which depends only upon the initial condition vortex separation and the conserved quantities. For example, two identical circular vortices of uniform like-signed vorticity merge when the initial centroid separation is smaller than 1.7 diameters.

Griffiths and Hopfinger [5] made laboratory experiments with geostrophic vortices in a two-layer density stratification. They showed that the combination of two vortices of opposite sign in different layers, called hetons, tear each other apart over a distance of order one Rossby radius or less, while they repel each other if separated by larger distance. They also observed that real vortices of like sign and in the same layer coalesce when they approach sufficiently close to each other. In another work Griffiths and Hopfinger [6] showed that a pair of two-dimensional vortices of like sign generated in a rotating fluid coalesce if the vortex centres are placed less than a critical distance apart. This critical distance is $(3.3 \pm 0.2) r_0$, where r_0 is the radius of a core having nonzero relative vorticity, in agreement with [4] results.

The interaction of two isolated lenslike eddies was examined with the aid of an inviscid nonlinear model by Nof [7]. The barotropic layer in which the lenses are embedded is infinitely deep so that there is no interaction between the eddies unless their edges touch each other. Using qualitative arguments (based on continuity and conservation of energy along the eddies edge) it is shown that, once the eddies become in touch, intrusions along the eddies peripheries are generated. As time goes on, these intrusions or «tentacles» become longer and, ultimately, the eddies are entirely converted into very long spirallike tentacles. These spiraling tentacles are adjacent to each other so that the final result is a *single* vortex containing the fluid of the two original eddies. It was speculated that the above process leads to the actual merging of lenslike eddies in the ocean. Collisions between isolated modons were examined for the quasi-geostrophic, barotropic equations by McWilliams and Zabusky [8]. For a range of parameters they observed «inelastic» effects including speed changes due to vorticity rearrangement, vorticity filamentation and modon «capture» or «fusion» in an overtaking collision.

All previous numerical and analytical studies examined the merging process between idealized vortices corresponding to patches of uniform vorticity. In this study we use instead realistic horizontal vortex structures as described by Olson [9] for cyclonic and Joyce [10] for anticyclonic rings. The rings are shown to have an interior velocity field in near-solid body rotation, surrounded by a front which exhibits a maximum in the gradient of the velocity and in the potential vorticity. In our study we use the horizontal velocity structure suggested by Olson [9] for cold rings. The invariance of the vorticity equation for $\{\psi, y\} \leftrightarrow \{-\psi, -y\}$ transformations allows one to deduce the merging dynamics of anticyclonic rings from the simulations of cyclonic

rings. Thus for our equations there is no qualitative difference in the merging rates of cyclonic and anticyclonic vortices.

In sect. 2 we describe the model parameters and the vorticity structure of the initial rings. In sect. 3 and 4 we present the numerical experiments with variations of initial conditions and of model parameters, respectively.

2. – Model description and initialization.

The model used for these numerical simulations is the Harvard Open Ocean Model [11]. It is a regional dynamical model that has been developed for realistic local dynamical studies of fundamental processes and real data initialization. The model utilizes the quasi-geostrophic (QG) equations which are appropriate for the mesoscale/synoptic variability in the ocean.

Our quasi-geostrophic equations utilize the Rossby number, defined as $(f_0 t_0)^{-1}$, where t_0 is a characteristic time scale for the problem and f_0 is the Coriolis parameter evaluated at the central latitude, θ_0, of the region of interest. The resulting pseudopotential barotropic vorticity equation is

$$\frac{\partial \zeta}{\partial t} + \alpha J(\psi, \zeta) + \beta \frac{\partial \psi}{\partial x} = F_{pqr}\,, \tag{1}$$

where

$$\zeta = \nabla^2 \psi \tag{2}$$

and the Jacobian is defined as

$$J(\psi, \zeta) = \frac{\partial \psi}{\partial x}\frac{\partial \zeta}{\partial y} - \frac{\partial \psi}{\partial y}\frac{\partial \zeta}{\partial x}\,.$$

The nondimensional parameters are

$$\alpha = \frac{V_0 t_0}{D}\,, \qquad \beta = \beta_0 D t_0\,,$$

where V_0 is a typical fluid velocity and D the horizontal scale of motion; β_0 is the β parameter defined as $\beta_0 = \partial f/\partial y|_{y=y_0} = (2\Omega/a)\cos\Theta_0$ where a is the radius of the earth, Ω is the rotation rate and Θ_0 the central latitude of the domain. We call ζ the *relative vorticity* to be distinguished from $\beta_0 y$, the planetary vorticity.

The right-hand side of eq. (1), F_{pqr}, is the schematic representation of the Shapiro filter of order p, applied q times and every r time steps to ζ [12, 13]. We choose $p = 4$, $q = 1$ and $r = 1$. This corresponds to an eight-order Laplacian operator plus mixed derivatives as shown in [13]. This filter removes small-scale vorticity which cascades from larger scales in nonlinear flows via two-dimensional or geostrophic turbulence processes [14, 15]. Physically the removal is necessary since small scales are not included in the quasi-geostrophic scaling, and the model viscosity should not affect the larger scales. Computationally, if vorticity accumulates on the two-gridpoint scale, the numerical instability will result.

The computational model has been calibrated by Haidvogel *et al.* [16] and Miller *et al.* [17]. It is finite element in the horizontal and the time evolution is calculated with an Adams-Bashford scheme. The open horizontal boundary conditions are those spec-

TABLE I. – *Model symbols, parameters and scaling factors. Adapted from* [20].

Symbols	Definitions
V_0	velocity scale = 40 cm/s
t_0	time scale = 4 days
D	horizontal scale = 40 km
f_0	Coriolis parameter at $\theta_0 = 39°$ N$(9.1 \cdot 10^{-5}$ s$^{-1})$
β_0	$\partial f/\partial y\|_{\theta=\theta_0} = 1.8 \cdot 10^{-11}$ (ms)$^{-1}$
α	$t_0 V_0/D = 3.456$
β	$\beta_0 t_0 D = 0.2558$

ified by Charney, Fjortoft and von Neumann [18], *i.e.* streamfunction specified everywhere on the boundary and vorticity specified at inflow points. The mathematical problem will be closed by the specification of an initial condition for ψ and ζ.

For the present purpose of modelling vortices, the side boundaries are specified as closed, *e.g.*, the streamfunction is imposed to be constant along the walls together with the initial vorticity. In order to find the numerical values of the model parameters α and β, we used the nondimensional time, space and velocity values listed in table I. The scales of motion were chosen to reflect the dynamics of the Gulf Stream system [19, 20]. Horizontal velocities are scaled by 40 cm/s, a typical particle speed in the main thermocline. The spatial scale of 40 kilometers is representative of the Rossby radius of deformation. The temporal scale of 4 days corresponds to the fastest time required for the evolution of a large meander. The horizontal resolution is 9 kilometers, the total domain is 131×81 gridpoints and the time step is half an hour.

The initial condition is represented by two equal cold (cyclonic) barotropic vortices whose initial separation distance d is measured from their centres surrounded by still water. Of course this quiescent ocean does not correspond to a realistic oceanic situation but it can be a reasonable approximation since rings immediately after birth have velocities at their rim much greater than the surrounding waters. In order to calculate the appropriate streamfunction and vorticity fields for model initialization, an analytic expression for the velocity structure of the two vortices is assumed. We use the «feature model» for Gulf Stream rings which has been used in ocean forecast experiments [20]. The tangential velocity increases linearly from zero at the centre out to a maximum $V_{\max}$ at a radius r_0:

$$v(r) = \frac{V_{\max}}{r_0} r \qquad \text{for } r < r_0 . \tag{3}$$

Outside r_0 the velocity decays exponentially:

$$v(r) = V_{\max} \exp\left[a\left(1 - \frac{r}{r_0}\right)\right] \qquad \text{for } r > r_0 . \tag{4}$$

The parameters of the vortex feature model are thus given by the maximum velocity $V_{\max}$, the radius of maximum velocity r_0 and the exponential decay factor a. A schematic of the vortex model and its associated parameters is shown in fig. 1*a*). The standard parameters for the vortices employed by McGillicuddy [21] and Robinson *et*

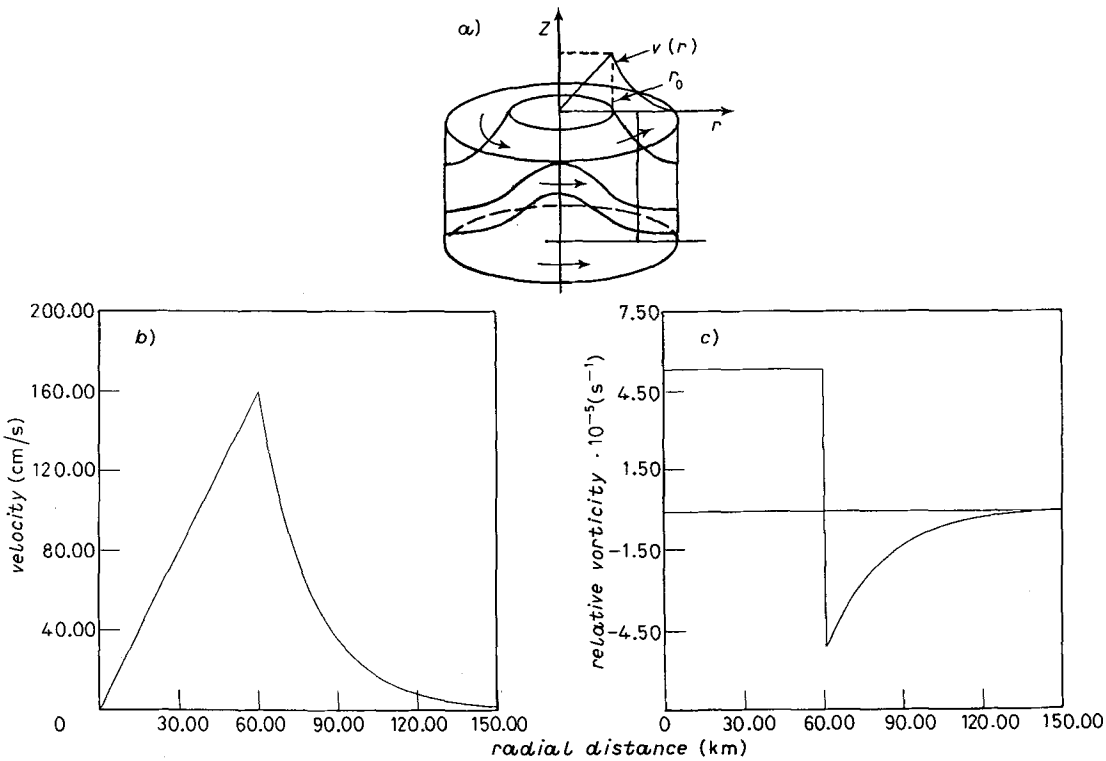

Fig. 1 – *a*) Schematic of a barotropic ringlike vortex structure developed by Robinson *et al.* [20]. *b*) Tangential velocity structure of rings as shown by Olson [9]. *c*) Relative vorticity as a function of radial distance.

al. [20] are

$$V_{\max} = 160\,\text{cm/s}\,, \qquad r_0 = 60\,\text{km}, \qquad a = 3\,.$$

From expressions (3) and (4) we can write the geostrophic streamfunction and vorticity fields for model initialization. The analytic streamfunction is written as

$$\psi(r) = \int \frac{V_{\max}}{r_0} r\,\mathrm{d}r = \frac{V_{\max}}{2r_0} r^2 + c_1 \qquad \text{for } r < r_0\,, \tag{5}$$

$$\psi(r) = \int V_{\max} \exp\left[a\left(1 - \frac{r}{r_0}\right)\right] \mathrm{d}r = -V_{\max} \frac{r_0}{a} \exp\left[a\left(1 - \frac{r}{r_0}\right)\right] + c_2 \qquad \text{for } r > r_0\,. \tag{6}$$

Assuming continuity in the streamfunction field we obtain $c_2 = (V_{\max}/2r_0)\, r_0^2 + (V_{\max}/a)\, r_0$ and we can choose $c_1 = 0$. We obtain the relative vorticity field calculating the Laplacian of the streamfunction in polar coordinates which results:

$$\zeta = 2\frac{V_{\max}}{r_0} \qquad \text{for } r < r_0\,, \tag{7}$$

$$\zeta = V_{\max} \exp\left[a\left(1 - \frac{r}{r_0}\right)\right]\left(-\frac{a}{r_0} + \frac{1}{r}\right) \qquad \text{for } r > r_0 . \tag{8}$$

In fig. 1*b*) and 1*c*) analytical velocity and relative vorticity profiles are shown. Equations (5)-(8) give the ψ and ζ fields associated to a cyclonic vortex for model initialization. We will use the superposition of two of these analytical expressions to initialize the model with two nearby vortices.

3. – Initial condition sensitivity experiments.

In table II we show a summary of the model runs. In this section we take into consideration only the experiments done with different initial conditions. The parameters used to change the initial fields are: the initial separation distance, d, between the two vortices measured from their centres and the maximum horizontal velocity of the vortex $V_{\max}$. The model parameters are left unchanged and equal to their standard values listed in table I. These first numerical simulations show the necessary conditions for the merger process without considering the characteristic of the oceanic environment (α, β) where they interact. For all the model runs described below, we show only the relative vorticity fields and all the experiments are carried out for 20 days earth time.

Figure 2 shows the evolution of the two vortices for experiment I1, which we call the «standard» experiment (see table II). After 4 days the two vortices have completely merged. This means that the initially distinct uniform vorticity fields (at the centre of the vortices) are now fused in a unique centre with a single positive maximum. After only two days it is interesting to notice the characteristic «S» shape of the forming vortex [4], *e.g.*, the combination of the two merging vortices and the developing arms at their opposite extremities. The arms are clearly due to a process of vorticity filamentation as a result of a two-dimensional turbulent cascade. Furthermore already at day 2 we can see the presence of two small vortices called «near-field» vortices in the upper left and lower right end of the S [2]. These «near-field» vortices are opposite-signed vorticity regions with respect to the vortex interior region, *i.e.* they are anticyclonic vortices if the initial interior vorticity field is cyclonic. They are located near the forming arms of the merging vortices. After 6 days of integration the vortex horizontal stretching is more obvious and the β-effect is clearly shown by the

TABLE II. – *Run table. The model parameter symbols are explained in table* I; $V_{\max}$ *represents the maximum vortex speed and d the vortices separation in* km *or multiple of* r_0.

Run name	Initial condition parameters		Nondimensional model parameters	
	d (km/r_0)	$V_{\max}$ (cm/s)	α	β
I1	144/2.4	160	3.456	0.2558
I2	144/2.4	100	3.456	0.2558
I3	126/2.1	160	3.456	0.2558
I4	162/2.7	160	3.456	0.2558
P1	144/2.4	160	3.456	0.0
P2	144/2.4	160	3.456	1.0
P3	144/2.4	160	0.0	0.2558
P4	144/2.4	160	1.0	0.2558

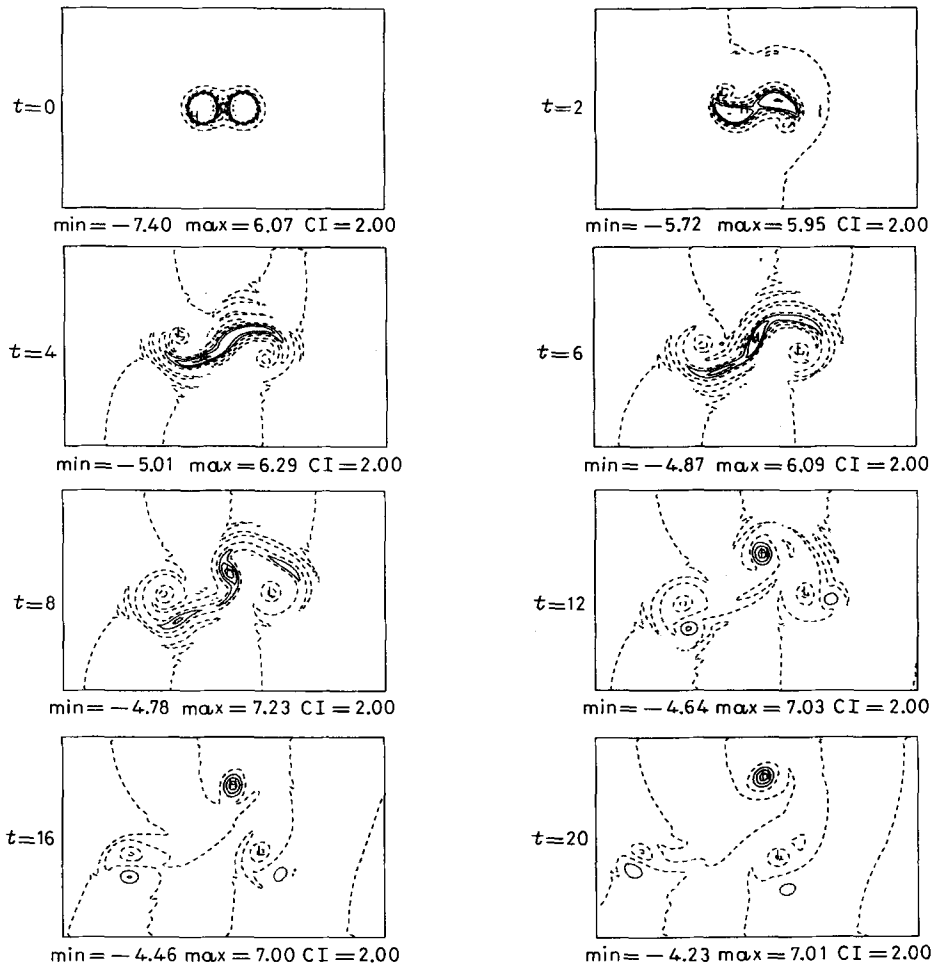

Fig. 2. – I1 standard experiment relative vorticity field. The time of integration is written on the left side and the maximum, minimum and contour interval used is displayed below each picture. Dashed contours correspond to negative values and continuous lines to positive values. The first dashed closed contour after a continuous line represents the zero contour level.

tendency of the left arm to move in the west direction faster than the right arm. We see the left arm already detaching a relative positive maximum in the vorticity field while the right arm contains little of the central vorticity of the merged vortex. After 8 days the previous vorticity structure has become unstable and part of the arms are cut off from the merged vortex. Two dipolar vorticity structures are then formed by the cut-off of the arm's vorticity and the near-field vortices. The central region of the merged vortex will evolve as a single monopole. After 12 days both the monopole and the dipoles become axisymmetric structures [22]. The two dipoles propagate westward because of the β-effect while the monopole moves northward as isolated cyclones do in order to conserve the sum of its relative and planetary vorticity [23].

To check that the numerical set-up does not affect qualitatively the results of experiment I1, we doubled both the horizontal resolution and the domain size. The re-

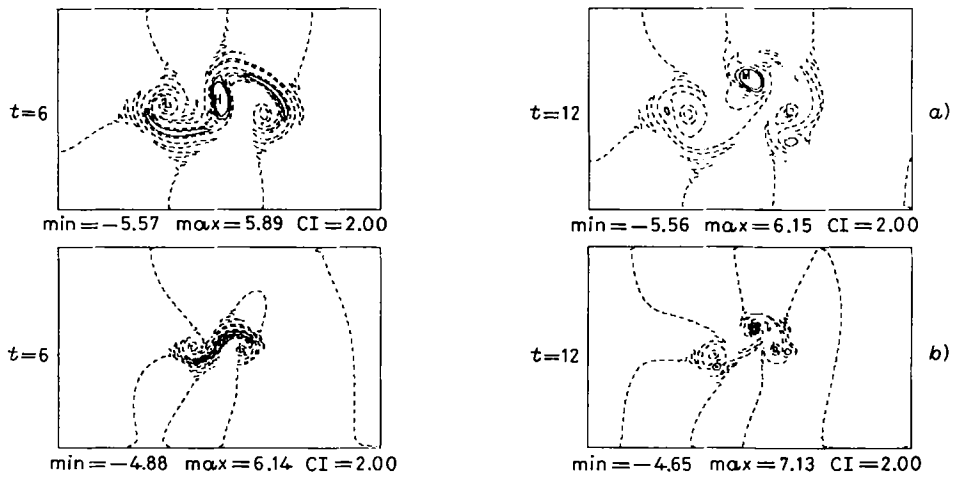

Fig. 3. – Comparison between double-resolution experimental (*a*)) and double-domain results (*b*)). The time in days is indicated on the left side.

sults are shown in fig. 3. Doubling the domain size has almost no quantitative impact on the solution, as we can see comparing fig. 3 with fig. 2 results. Changing the horizontal resolution to 4.5 km does not affect the qualitative behaviour of the solution, *e.g.*, the merging speed of the two initial vortices. However it changes the rotation speed of the merger vortex and of the dipoles. Furthermore the time of merging of the vortices does not change (day 4). Of course we changed the filter to be fourth order, applied 17 times each time step. This causes the spectral properties of the filter applied to I1 and to the double-resolution run to be approximately the same [21]. In the following we retained the resolution of 9 km for all the runs.

The evolution of experiment I2 (see table II), done with lower initial maximum velocity of the rings, is shown in fig. 4. After 2 days of integration we can clearly see that the two initial vortices are interacting but the «S» shape of experiment I1 is not as pronounced. After 4 days the central regions of the two initial vortices are coming into contact but they have not merged yet. The merging process will be complete only after 5 days (not shown). Thus the decrease in the vortex maximum velocity slows down the merging rate. At the eighth day the merged vortex is horizontally straining and after 12 days we can see that only the left arm is parting from the vortex because of the β-effect. After 16 days the detached arm and its «near-field» vortex form a dipolar structure while the single vortex developed from the merging process has assumed again an isolated and axisymmetric shape. The slower merging is the cause of larger breaking arm asymmetry with respect to the I1 case. Furthermore the smaller initial curvature ($t=2$ and $t=4$ in fig. 4) of the forming «S» at the arm ends provoques the formation of weaker near-field vortices. Thus it is possible to speculate that the near-field vortices are formed as a mechanism to equilibrate locally the increase in curvature of the vorticity field. In other words, a horizontal vorticity redistribution process is triggered to balance for the local increase of vorticity accumulating in the arms and it produces the closed circulations of the near-field vortices. If vertical vortex stretching (baroclinicity) is present, we can speculate that the near-field vortices could be not as strong as in the fully barotropic case because relative vorticity could

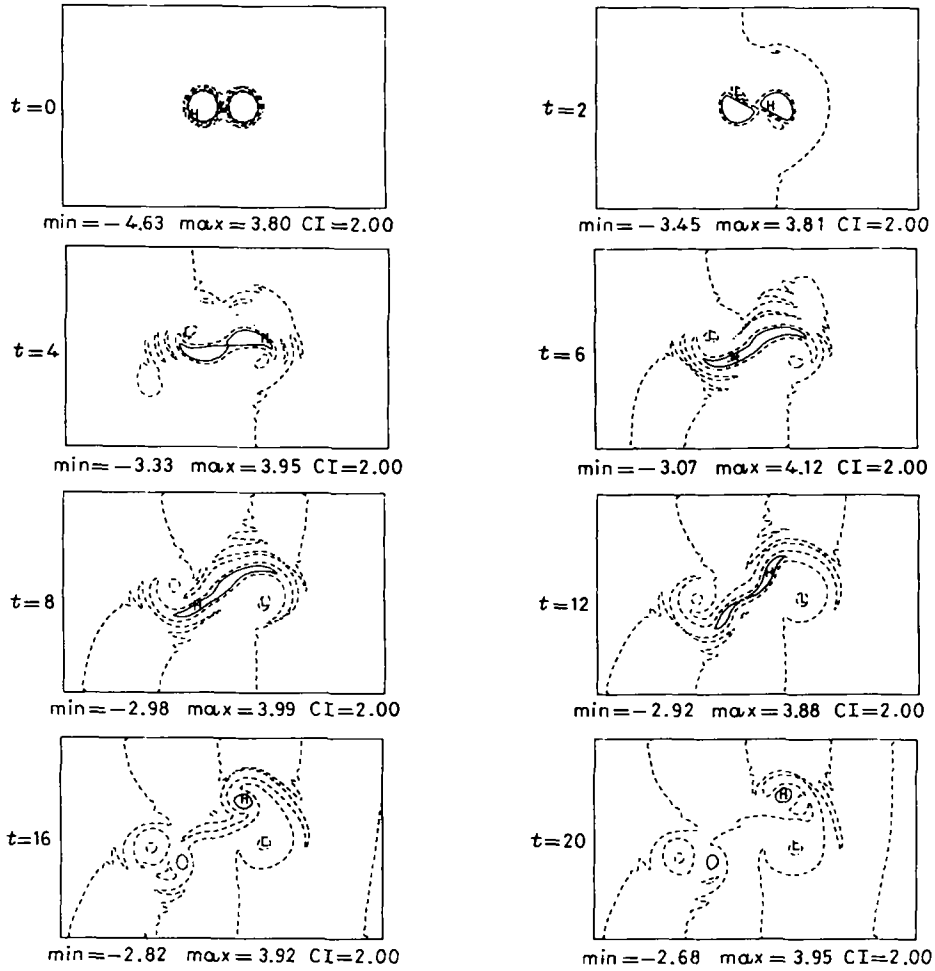

Fig. 4. – As in fig. 2 but for the I2 case.

be transformed into stretching vorticity without triggering the horizontal redistribution process. Furthermore this experiment indicates that vortex merging is a nonlinear barotropic instability process as found by [1, 6] and [24]. In fact the increase of the maximum horizontal shear (V_{max}) does speed up the merging as expected if shear instability is a controlling factor for merging.

In fig. 5 we compare experiments I3 and I4 (see table II) done with different initial distances between the vortices. After 2 days, in the case of small d, the two initial vortices have just merged while, in the case of large d, they are interacting but far from merging. At the fourth day the merged vortex has the characteristic «S» shape but it is rotated with respect to the standard case I1 and the straining arms are much different since of their different north-south displacement and the β-effect. The two vortices in the right column are also unstable and develop into elliptic shaped vortices but it is clear that they will not merge. Two-dimensional turbulent cascade develops also in this case and thus the «near-field» vortices form to equilibrate for the

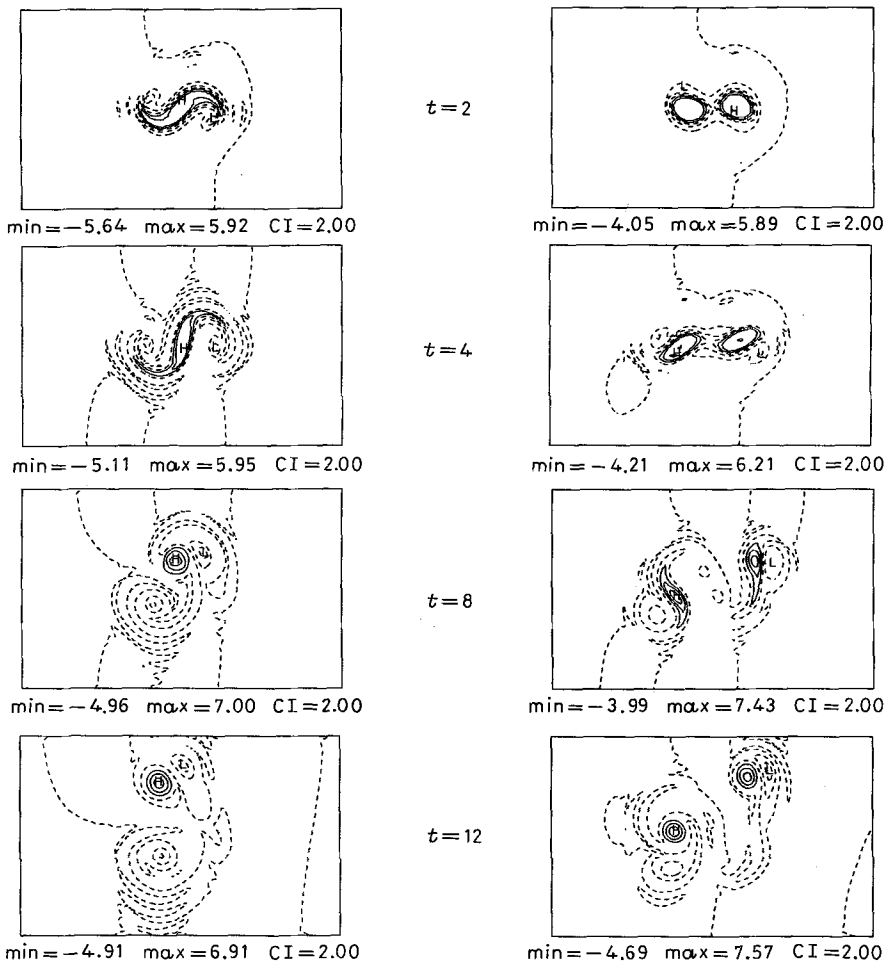

Fig. 5. – Left column: relative vorticity field for I3 experiment; right column: relative vorticity field for I4 experiment. Time in days is displayed at the centre. The contour conventions are described in fig. 2.

filamenting arms. In experiment I3, at day 8, the arms in the merged vortex are going to cut off and the central vorticity region assumes an axisymmetric shape again. However there is very little vorticity in the arms and the cut-off is practically filtered out leaving the «near-field» vortex as a monopole. Due to the different rotation rate and orientation of the merged vortex, the latter interacts with the near-field vortex at the right and couples with it, forming a dipole. The two vortices in the right column are rotating on themselves counter-clockwise and their «near-field» vortices interact with the initial core of the vortex forming two dipolar structures. The evolution of each vortex in the nonmerging case looks like a single vortex evolution [21, 23].

Comparing the «standard» case I1 with I3 it is clear that a greater initial separation distance between the vortices decreases the rate of the merging process. On the other hand, the process cannot happen if the initial distance is greater than the criti-

cal distance $d = 2.4\,r_0 \pm 2\,\Delta x = (2.4 \pm 0.3)\,r_0$. Melander *et al.* [4] obtained a critical distance $d = 3.4\,r_0$ which was confirmed by a value of $(3.3 \pm 0.2)\,r_0$ found by Griffiths and Hopfinger [6].

In synthesis, we have shown that, in order to have a merging process between two ringlike symmetric vortices, they must be separated by a critical distance. The time length of the initial interaction is controlled by the value of the maximum velocity. The duration of the initial phase of merging determines the behaviour and the development of the arms and «near-field» vortices. The «near-field» vortices are the result of a local horizontal redistribution process due to the increase in curvature of the vorticity field of the arms which are formed by two-dimensional turbulence cascade of enstrophy. Furthermore the arms are unstable and they can get detached from the central vortex forming dipolar structures with the «near-field» vortices.

4. – Sensitivity experiments.

In order to study the physical processes that affect merging rates with no dependence on initial conditions, we describe the numerical experiments done with the variation of: β, the parameter responsible for Rossby wave propagation and α, the nonlinear parameter. In table II the different runs are described. Here of course the initial condition is held constant and equal to the standard case I1.

The evolution of the two vortices with different values of the β parameter is shown in fig. 6. The comparison is made between the P1 and P2 case. After 2 days the two initial vortices are interacting in both cases at the same speed and the «near-field» vortices are present. The difference between the two experiments is visible in the Rossby wave packets emanating from the vortex and in the asymmetric development of the right vortex in the case $\beta = 1.0$ (P2 case). At the fourth day the merging process is nearly complete even though in both cases it is slower than the standard case I1. In the P1 case the characteristic arms are completely symmetric while in the case P2 the greater westward stretching of the left arm is clearly visible. This asymmetric behaviour of the arms caused by the β-effect is stronger in this case than in the «standard» I1 one because of the greater β value. Furthermore in the P2 case the «near-field» vortices seem to depart from the arms and have a separate evolution from the fourth day. At day 8 the arms are cut off from the merged vortex symmetrically in P1 in contrast with the P2 case. The difference becomes larger after 12 days where the P1 case shows two dipolar vorticity structures formed by the «near-field» vortices and the vorticity cut-off from the arms, while the P2 case shows five isolated monopoles formed by the merger, the near-field vortices and cut-off arms vorticity. Thus a strong β-effect breaks the interaction between the arms and the near-field vortices allowing their separate evolution. This parameter sensitivity experiment shows that β-effect does not alter appreciably the speed of the merging process but changes the dynamics of the interaction and the development of the arms totally.

The last two numerical experiments compare the evolution of the two vortices with different α values. The P3 and P4 cases are shown in fig. 7. In the P4 case the two vortices begin to interact after 2 days while in the P3 case the ring positive vorticity maxima seem to repel and move both westward. At day 4 the vortices in the P4

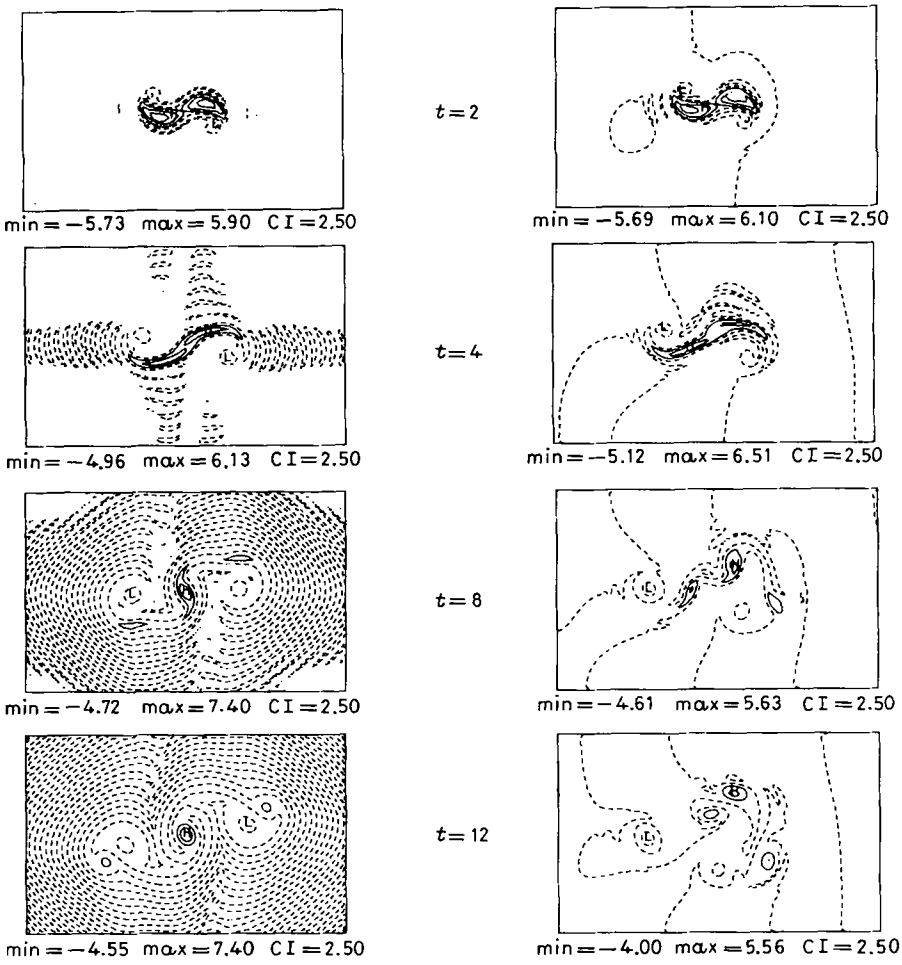

Fig. 6. – Left column: relative vorticity field for experiment P1; right column: relative vorticity field for experiment P2. Time in days is displayed at the centre. The contour conventions are described in fig. 2.

case are interacting producing a typical «S» shape area while the vorticity field in the P3 case will continue until the end to develop a westward intensification of the central ring vorticity with some Rossby wave packet propagation emanating from the left side of the vortices. In the P4 case the merging occurs at day 8 but no arms get detached from it even later in the integration. In conclusion P3 and P4 experiments show that the merging process is halted by low values of the α parameter together with all the interaction phenomena as the deformation, the rotation and the stretching of the vorticity field. In both linear (P3) and weak nonlinear cases (P4) the northward displacement of the merging structures is absent or slower. This result agrees with McWilliams and Flierl [23] conclusion that the nonlinear terms produce a net northwestward propagation effect at a rate about twice than that due solely to the β term.

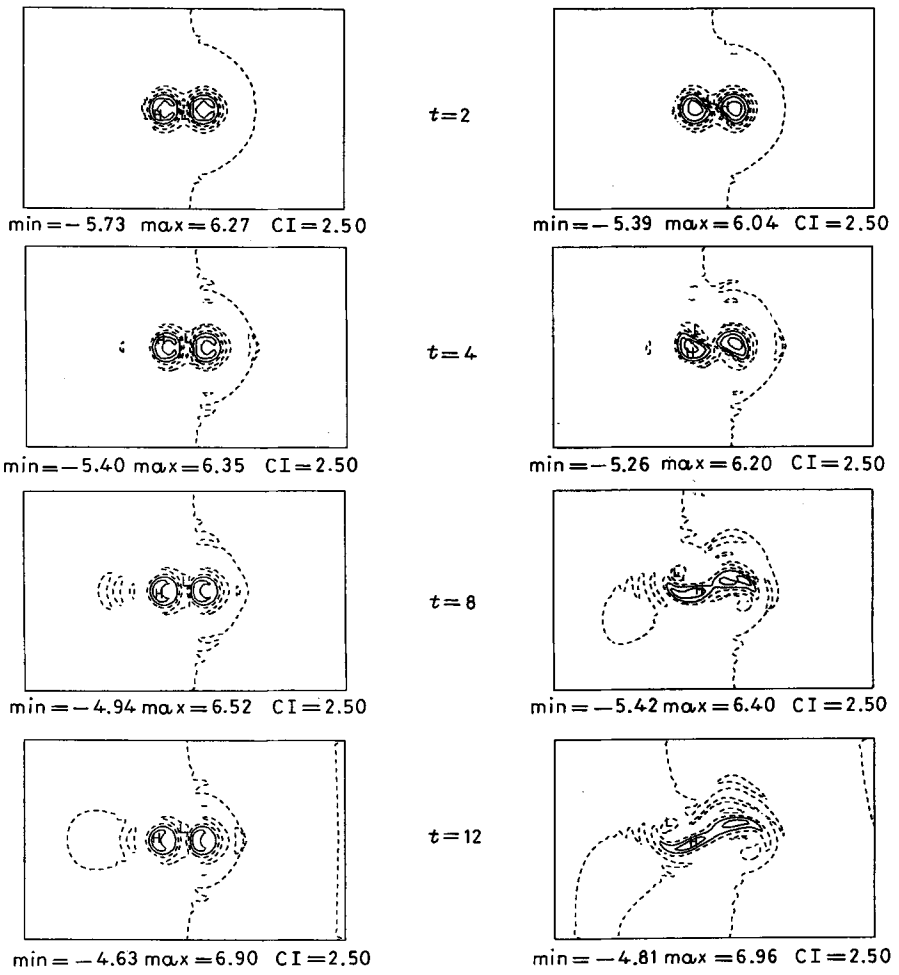

Fig. 7. – Left column: relative vorticity field for experiment P3; right column: relative vorticity field for experiment P4. Time in days is displayed at the centre. The contour conventions are described in fig. 2.

5. – Conclusions.

In this paper we have presented the numerical simulations of axisymmetric ring-like vortex interactions in order to study the importance of initial vortex strength and environmental parameters in the merging process.

We observed that interaction and merging rate depend strongly on the initial conditions and that the development of arms and «near-field» vortices depends on the nondimensional parameters of the model. A necessary condition for merger is that the initial separation distance between the vortices, d, is smaller than the critical value of $(2.4 \pm 0.3) r_0$ and that the nonlinear parameter α is nonzero. A lower value of V_{max} slows down the merging rate and the rotation speed of the merged structure. We can argue that a lower V_{max} value means a smaller nonlinear instability of the merging structure and thus a slower merging rate. This result is in agreement with the inter-

pretation of the merger process as a finite-amplitude barotropic instability process as found in realistic merging of oceanic vortices [1, 6] and [24]. We also verified that nonlinear terms represent a net northward propagation tendency for cyclonic vortices.

The β parameter is not a necessary condition for merging to occur but it changes the development of the arms and «near-field» vortices. It is important to notice that both small ($\beta = 0.$) and large ($\beta = 1.$) β values slow down the merging. Perhaps the most interesting result of this study is contained in the analysis of «near-field» vortices and associated cut-off arms. The «near-field» vortices seem to be associated to a barotropic redistribution process around the filamenting arms. Furthermore the «near-field» vortices can depart from the arms when β is strong and have a separate life.

We also observed that the interaction-time between vortices determine completely the behaviours of «near-field» vortices and arms. After the merging the arms of the new vortex become unstable. When the process of merging is not too fast or too slow, they can get detached from the central vortex to form dipolar structures with «near-field» vortices. We have shown the formation of both dipolar and monopolar structures as a result of the interaction between the «near-field» vortices and the arms of the merged vortex. The formation of these structures depends on the detailed form of the initial condition and the environmental parameters. It is clear that, in the «realistic» parameter range value for Gulf Stream rings, the merging rate is fast (~ 4 days) and the dipolar structures can form as a result of arms cut-off and near-field vortices interaction.

Our results basically agree with those of Griffiths and Hopfinger [6] who used similar interacting vortices in a water tank but did not explore the dynamics of arms and near-field vortices.

We are now extending these results to the baroclinic case and the preliminary results show that the «near-field» vortices are weaker than in the purely barotropic case. This confirms that the dynamical balance responsible for the «near-field» vortex formation is essentially a horizontal nonlinear redistribution of vorticity caused by the local increase in the curvature vorticity of the forming arms.

* * *

We are thankful to Dr. Santoro, thesis supervisor, Dr. Guzzi and Dr. Navarra for enthusiastic support of this work. This work has been financed by a grant of the Progetto Finalizzato «Calcolo Parallelo».

REFERENCES

[1] A. R. ROBINSON, J. A. CARTON, N. PINARDI and C. N. K. MOOERS: *J. Phys. Oceanogr.*, **16**, 1561 (1986).
[2] J. P. CHRISTIANSEN and N. J. ZABUSKY: *J. Fluid Mech.*, **61**, part 2, 219 (1973).
[3] E. A. OVERMAN and N. J. ZABUSKY: *Phys. Fluids*, **25**, 1297 (1982).
[4] M. V. MELANDER, N. J. ZABUSKY and J. C. MCWILLIAMS: *A model for symmetric vortex-merger* in *Transactioms of the Third Army Conference on Applied Mathemtics and Computing*, ARO Report 86-1, 1985.
[5] R. W. GRIFFITHS and E. J. HOPFINGER: *J. Fluid Mech.*, **173**, 501 (1986).

[6] R. W. GRIFFITHS and E. J. HOPFINGER: *J. Fluid Mech.*, **178**, 73 (1987).
[7] D. NOF: *J. Phys. Oceanogr.*, **18**, 887 (1987).
[8] J. C. MCWILLIAMS, and N. J. ZABUSKY: *Geophys. Asytrophys. Fluid Dynamics*, **19**, 207 (1982).
[9] D. B. OLSON: *J. Phys. Oceanogr.*, **10**, 514 (1980).
[10] T. M. JOYCE: *J. Phys. Oceanogr.*, **14**, 936 (1984).
[11] A. R. ROBINSON and L. J. WALSTAD: *J. Appl. Numer. Math.*, **3**, 89 (1987).
[12] R. SHAPIRO: *Rev. Geophys. Space Phys.*, **2**, 491 (1970).
[13] R. SHAPIRO: *J. Atmos. Sci.*, **28**, 523 (1971).
[14] P. B. RHINES: *Annu. Rev. Fluid Mech.*, **11**, 401 (1979).
[15] J. PEDLOSKY: *Geophysical Fluid Dynamics* (Springer-Verlag, 1979).
[16] D. B. HAIDVOGEL, A. R. ROBINSON and E. E. SCHULMAN: *J. Comput. Phys.*, **34**, 1 (1980).
[17] R. N. MILLER, A. R. ROBINSON and D. B. HAIDVOGEL: *J. Comp. Phys.*, **50**, 38 (1983).
[18] J. G. CHARNEY, R. FJORTOFT and J. VON NEUMANN: *Tellus*, **2**, 237 (1950).
[19] N. PINARDI: *Quasigeostrophic-Energetics and Ocean Mesoscale Dynamics*, Thesis for the degree of Doctor of Philosophy in Applied Sciences, Harvard University, Cambridge, USA (1985).
[20] A. R. ROBINSON, M. A. SPALL and N. PINARDI: *J. Phys. Oceanogr.*, **18**, 1811 (1988).
[21] D. J. MCGILLICUDDY: *Quasigeostrophic Modelling of Isolated Vortices*, Thesis for the degree of Bachelor of Arts in Engeneering Sciences, Harvard University, Cambridge, USA (1987).
[22] J. C. MCWILLIAMS: *J. Fluid Mech,*, **146**, 21 (1984).
[23] J. C. MCWILLIAMS and G. R. FLIERL: *J. Phys. Oceanogr.*, **9**, 1155 (1979).
[24] N. PINARDI and A. R. ROBINSON: *Dyn. Atmos. Oceans*, **10**, 185 (1986); **18**, 1811 (1986).